

Analytical Solution for Turbulent Flow in Channel

Date: July 10, 2023

Alex Fedoseyev
Ultra Quantum Inc., Huntsville, Alabama, USA
Email: af@ultraquantum.com

Abstract

In this work the exact and approximate analytical solution of the GHE for turbulent flow in channel are presented. It was discovered first by numerical simulations, Fedoseyev and Alexeev (2010), and now the explicit formula are obtained. The solution is a superposition of the laminar (parabolic) and turbulent (superexponential) solutions. The analytical solution compares well with the experimental data by Van Doorne (2007) for axial velocity and data by Nikuradse (1933) for axial velocity, for flows in pipes.

It is proposed to explain the nature of turbulence as oscillations between the laminar (parabolic) and turbulent (superexponential) solutions. Good comparison of the analytical formula, a difference of the parabolic and superexponential solutions, for turbulent velocity fluctuations with the experiment by Van Doorne (2007) confirmed this suggestion. The Navier-Stokes equations do not have the superexponential solution.

The obtained analytical solution provides a complete structure of the turbulent boundary layer that compares well with the experiments by Wei and Willmarth (1989). It also presents an explicit verifiable proof that Alexeev's generalized hydrodynamic theory (GHE) is in close agreement with experiments for turbulent flows.

1 Introduction

Generalized Hydrodynamic Equations (GHE) have been proposed by Boris Alexeev (1994)[1]. They were used for the simulations of incompressible viscous flows for a wide range of problems and flow parameters, including high Reynolds number turbulent flows with thin boundary layers in 3D driven cavity flow at $Re = 3200$ and $10,000$, 2D backward facing step flow at $Re = 132,000$, flow in channels for Reynolds number up to $Re = 10^6$, magnetohydrodynamic flows [7, 8, 9, 10, 12], resulting in good agreement with experiments [20], [19] and other works.

GHE model has been applied to compressible hypersonic flows that exhibit both continuum and non-continuum flow regimes. The shock wave (bow shock) can be detached from the vehicle at high altitude, and near boundary slip-flow is typical for such regimes. Results for hypersonic GHE model have been reported in [13, 14, 15] are in close agreement with the experiments by [3, 17, 18] and other works even for highly rarefied flows.

In this work an approximate analytical solution of GHE for turbulent flow in channel is presented and compared with the experimental data.

Generalized Hydrodynamic Equations (GHE) are based on a new set of conservation equations obtained from a generalized version of the Boltzmann equation (GBE) by Alexeev that includes

more details of the molecular collision processes [1], [2]. The model combines continuum-to-free molecular flow physics in one consistent formulation by accounting for the kinetic effects (intermediate Knudsen number, fluctuations and turbulence) in the continuum approximation. A brief outline of the basic ideas of GBE and derivation of governing Generalized Hydrodynamic Equations is presented in Section 1.1.

1.1 Generalized Boltzmann Transport Equation (GBE)

Physical derivation of the standard Navier-Stokes equations (NS) can be obtained from the kinetic theory of gases, which is based on the solution to the Boltzmann transport equation for space-time evolution of particle velocity distribution function, f , written in the form

$$\frac{Df}{Dt} = J, \quad (1)$$

where D/Dt represents material derivative in space, velocity space and time and J is the collision integral. The standard Boltzmann transport equation takes into account the changes in distribution function f on hydrodynamic and mean time between collision time scales of infinitesimal particles. Accounting for a third time scale associated with finite dimensions of interacting particles gives rise to an additional term in the Boltzmann transport equation resulting in a generalization of the form as

$$\frac{Df}{Dt} - \frac{D}{Dt}(\tau^* \frac{Df}{Dt}) = J, \quad (2)$$

where τ^* is the mean time between particle collisions. The new term is thermodynamically consistent and is proportional to the Knudsen number, Kn , and therefore in the hydrodynamic limit, to viscosity. More details on the GBE are provided in the Alexeev's book [2].

2 Generalized Hydrodynamic Equations

Hydrodynamic equations can be obtained from Eq. (2) by multiplying the latter by the standard collision invariants (mass, momentum, energy) and integrating the result in the velocity space. These equations are for incompressible viscous flow, presented originally in [12], are the following:

$$\frac{\partial \mathbf{V}}{\partial t} + (\mathbf{V}\nabla)\mathbf{V} - Re^{-1}\nabla^2\mathbf{V} + \nabla p - \mathbf{F} = \tau \left\{ 2\frac{\partial}{\partial t}(\nabla p) + \nabla^2(p\mathbf{V}) + \nabla(\nabla \cdot (p\mathbf{V})) \right\} \quad (3)$$

while continuity equation is

$$\nabla \cdot \mathbf{V} = \tau \left\{ 2\frac{\partial}{\partial t}(\nabla \cdot \mathbf{V}) + \nabla \cdot (\mathbf{V}\nabla)\mathbf{V} + \nabla^2 p - \nabla \cdot \mathbf{F} \right\} \quad (4)$$

where \mathbf{V} and p are nondimensional velocity and pressure, $Re = V_0 L / \nu$ - the Reynolds number, V_0 - velocity scale, L - hydrodynamic length scale, ν - kinematic viscosity, \mathbf{F} is a body force and a nondimensional $\tau = \tau^* L^{-1} V_0$. Note that the right-hand side of (3) is the divergence of the fluctuation part of flow velocity, expressed explicitly through original primitive variables according to [1].

We made the following assumptions deriving Eq. (3, 4):

- τ is assumed to be constant,
- Neglected the nonlinear terms of the third order in the fluctuations, and terms of the order τ/Re and smaller,
- Assumed slow flow variation, so neglect second derivatives in time.

Additional boundary conditions on walls are for fluctuations to be zero. The boundary condition for pressure on walls is

$$(\nabla p - \mathbf{F}) \cdot \mathbf{n} = 0, \quad (5)$$

where \mathbf{n} is a wall normal.

Note, that the dimension of a product $\tau^*\nu$ is a square of length. We introduce fluctuation length scale l , $l^2 = \tau^*\nu$ and rewrite nondimensional τ as $\tau = l^2 L^{-2} Re = K \cdot Re$, where $K = l^2/L^2$. The value of τ^* is a material property and not known in advance, but we provide speculation on a choice of τ^* value in Section 5 and in the discussion of results, Section 7.

The obtained GHE model is not a turbulence model, and no additional equations are introduced. Kinetic effects (small flow scales) have been successfully captured with the GHE, and the obtained small scale of turbulence compared well with observations in experiments by Koseff and Street (1984) [20], and 2D and 3D Navier-Stokes solutions and $k-\varepsilon$ turbulent model solutions have been outperformed by GHE results, Fedoseyev and Alexeev (2012)[12].

In this paper to obtain the analytical solution we further simplify the GHE equations: (a) temporal derivatives are neglected in the fluctuations, (b) the nonlinear terms are neglected in the fluctuations.

2.1 Governing Equations for 2D Incompressible Flow

The case of 2D incompressible fluid flow is considered. The equations are taken from [12] where they are presented explicitly, and further simplification is done by dropping all the terms (with coefficient τ) in momentum equations, and keeping only Laplacian term in the continuity equation.

The resulting continuity equation of GHE model is the following:

$$u_x + v_y = \tau \nabla^2 p \quad (6)$$

while the momentum equations are :

$$u_t + u u_x + v u_y + p_x = Re^{-1} \nabla^2 u \quad (7)$$

$$v_t + u v_x + v v_y + p_y = Re^{-1} \nabla^2 v \quad (8)$$

where $Re = LV_0/\nu$ is Reynolds number, L is the length scale, V_0 is velocity scale, ν is kinematic viscosity, $\tau = \tau^*V_0/L$ is the nondimensional time scale from GHE (τ^* is the dimensional time).

One may point out that the continuity Eq. (6) is not correct, and the mass is not conserved for incompressible fluid (may have sources and sinks). Let us note, that

- Eq.(6), as well as Eq.(7, 8) are obtained by a the standard procedure, by multiplying Eq. (2) by standard collision invariants (mass, momentum, energy) and integrating the result in the velocity space. Then the simplification was done, and only the highest derivative was left in Eq. (6).

- Recall that the particles now are not the material points, but finitely-sized particles, that may be partially in and partially out of any control volume, and that is the origin of GBE, and the pressure Laplacian term in Eq.(6).
- When solving Eq.(6, 7, 8) numerically [11], the residuals of solution of Eq.(6) with Laplacian term and without that term have been verified. The residuals have been small and of the same order of magnitude in both cases, so no sources and sinks have been observed for wide range of flows. oth cases, so no sources and sinks have been observed for wide range of flows. Still the results using the Navier-Stokes equation with $\text{div}(\mathbf{V})=0$ were far from the experimental data while the GHE results with Eq.(6) fit the experimental data well [11].

3 Laminar Flow Solution

The 2D channel flow problem: a stationary flow in x direction in a 2D (horizontal) channel of width L with a center line velocity V_0 is considered. So the time derivatives are dropped in Eq.(7, 8). We consider the flow where everything is the same in any x cross section, so all the partial derivatives in x are zero, except for the applied pressure gradient p_x . The boundary conditions are:

$u = 0, v = 0$ and the normal derivative of the pressure $p_n = 0$ at the walls $y = 0$, and $y = L/2$. A flow with $p_x = \text{const}$ has a parabolic velocity u profile:

$$\begin{aligned} p_x &= Re^{-1} u_{yy}, \\ u_y &= Re p_x y + C_1 \\ u &= \frac{1}{2} Re p_x y^2 + C_1 y + C_2. \end{aligned}$$

Taking into account the boundary conditions, the laminar flow solution is

$$U_L = u(y) = 4V_0 y(L - y)/L^2, \quad (9)$$

where $V_0 = -\frac{1}{8} Re p_x L^2$, and $v = 0$ everywhere.

This solution of Eq.(6),(7),(8) is also a solution of the Navier-Stokes equations, as $\nabla^2 p = 0$.

The equations (6),(7),(8) also have a second solution, that was initially discovered numerically for a flow in 2D channel by Fedoseyev and Alexeev (2012) [11], Figure 1(a): both turbulent and laminar numerical solutions are shown for $Re = 5000$.

In this paper the second solution is obtained analytically, it is called as a turbulent solution, and it is a super exponential function:

$$U_T = V_0 \left(1 - e^{1 - e^{y/\delta}} \right). \quad (10)$$

Figure 1(b) shows example of both U_L (Eq.(9), parabolic, green line) and U_T (Eq.(10), super exponential, blue line) solutions for laminar and turbulent flows respectively.

In Section 4 it is explained how to obtain this approximate analytical solution (second solution). The construction of general solution of GHE is proposed in Section 5, and a comparison of this analytical solution with the experimental data is provided in Section 6.

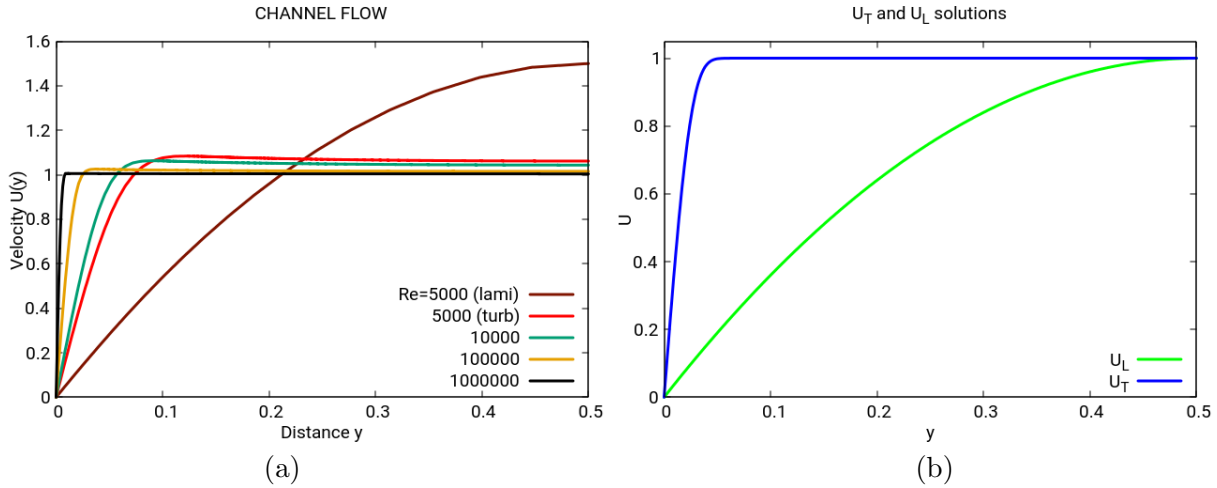


Figure 1: (a) Simulation of 2D channel flow where the turbulent solution has been discovered, Fedoseyev and Alexeev (2012) [11]: horizontal velocity $U(x)$, for $Re = 5 \cdot 10^3$ both laminar and turbulent solutions are shown (the brown and red lines), $10^4, 10^5$ and 10^6 (each solution has the same total flux). (b) Example of solutions for laminar and turbulent flows, U_L , Eq.(9) (parabolic solution, green line), and U_T , Eq.(10) (super exponential solution, blue line).

4 Analytical Solution of GHE

4.1 Exact Solution of GHE

A general solution can be constructed from a particular solution of a problem with non-zero right hand side (pressure gradient) and general solution with zero pressure gradient. Below, it is described how to find a second solution of GHE and then obtain a general solution.

We consider stationary flow regime

$$u u_x + v u_y + p_x = Re^{-1}(u_{xx} + u_{yy}) \quad (11)$$

$$u v_x + v v_y + p_y = Re^{-1}(v_{xx} + v_{yy}) \quad (12)$$

$$u_x + v_y = \tau(p_{xx} + p_{yy}) \quad (13)$$

Let us designate $\alpha = Re^{-1}$ and assume $u_x = v_x = 0, p_x = \text{const}$.

Then Eq.(12, 13) become

$$p_x = \alpha v_{yy} - v u_y \quad (14)$$

$$\tau p_{yy} = v_y \quad (15)$$

Integrating Eq.(15) one obtain

$$\tau p_y = v + C_1 \quad (16)$$

As $p_y = 0, v = 0$ at the wall, then $C_1 = 0$. Substitute that in Eq.(14) we get

$$\alpha v_{yy} - v v_y - v/\tau = 0 \quad (17)$$

The analytical solution of Eq.(17) is available (e.g. [23], Sec.2.2.3-2, Eq.2, and Sec.1.3.1-2 Eq.1, or WolframAlpha.com) in implicit form as Eq. (18),

$$y + C_2 = - \int_1^{v(y)} \tau / (W(-e^{-\tau(\xi^2 + 2\alpha\tau C_1)/(2\alpha) - 1}) + 1) d\xi \quad (18)$$

where $W(z) = W[k, z]$ is Lambert W function (or the Product Log function), the solution for w in $z = w \exp(w)$. Constants C_1 and C_2 are chosen to satisfy boundary conditions. There is the $k - th$ solution of the Eq.(17) corresponding to $W[k, z]$ in Eq.(18). There are multiple solutions of $v(y)$, and then multiple solutions $u(y)$ can be found by substituting $v(y)$ into Eq.(11). The pressure can be found using Eq.(16). This can not be done analytically to obtain the explicit formulas for $u(y)$ and $p(y)$. The example of solutions for $v(y)$ and $u(y)$ are shown in Figure 2.

In the Section 4.2 we obtain explicit analytical expressions for the approximate solution.

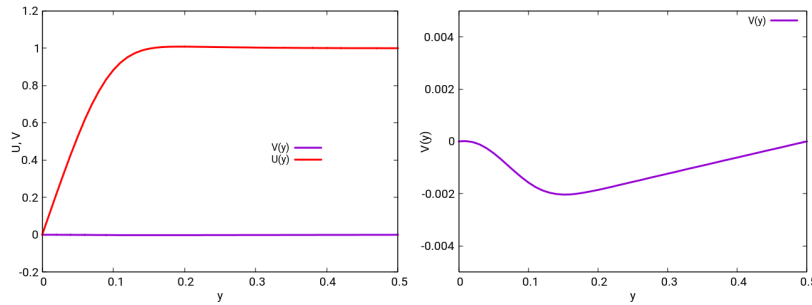


Figure 2: Example of the exact solution $v(y)$ for some C_1, C_2 of Eq.(18), and $u(y)$ from Eq.(11): (a) $u(y), v(y)$; (b) $v(y)$ details are shown.

4.2 Approximate Solution of GHE

Let us designate $\Psi = v_y$, $\alpha = Re^{-1}$ and assume $u_x = v_x = 0, p_x = \text{cont}$, and neglect small $v v_y$ term. Then

$$p_x = \alpha u_{yy} - v u_y \quad (19)$$

$$p_y = \alpha \Psi_y \quad (20)$$

$$\tau p_{yy} = \Psi \quad (21)$$

Substituting Eq.(20) into Eq.(21) obtain

$$\alpha \tau \Psi_{yy} = \Psi, \text{ or}$$

$$\alpha \tau \Psi_{yy} - \Psi = 0.$$

The solution is $\Psi = A e^{\pm \frac{y}{\sqrt{\alpha\tau}}}$, and recalling what is Ψ :

$v_y = A e^{\pm \frac{y}{\sqrt{\alpha\tau}}}$, integrating that one obtains:

$v = A_1 e^{\pm \frac{y}{\sqrt{\alpha\tau}}} + B_1$, then applying boundary condition:

$v = 0$ at $y=0$, obtain the solution v :

$$v = A(1 - e^{\pm \frac{y}{\sqrt{\alpha\tau}}}), \quad (22)$$

Here

$$\alpha \tau = \tau Re^{-1} = \frac{\tau^* V}{L} \cdot \frac{\nu}{VL} = \frac{\tau^* \nu}{L^2} = \delta^2,$$

or

$$\delta = \frac{\sqrt{\tau^* \nu}}{L} \quad (23)$$

4.3 Case of the Positive Sign in the Exponent

In this case the solution for $v = A(1 - e^{y/\delta})$ grows exponentially, still for $y \leq L/2$ it is limited. So we try to get the solution u using obtained solution for v . Let us recall Eq.(19) and put the solution for v there, we have:

$\alpha u_{yy} - A(1 - e^{y/\delta})u_y - p_x = 0$, where $p_x = 0$, as we search for a solution of a homogeneous equation

$$\alpha u_{yy} - A(1 - e^{y/\delta})u_y = 0, \quad (24)$$

To integrate once in y we rewrite Eq.(24) as:

$$\frac{u_{yy}}{u_y} = \frac{A}{\alpha}(1 - e^{y/\delta}),$$

and obtain integral as

$$\ln u_y = \frac{A}{\alpha}(y - \delta e^{y/\delta}) + C_1$$

or

$$\ln u_y = \frac{A\delta}{\alpha}(y/\delta - e^{y/\delta}) + C_1$$

or

$$u_y = \exp\left(\frac{A\delta}{\alpha}(y/\delta - e^{y/\delta}) + C_1\right) \quad (25)$$

The explicit expression for the solution of $u(y)$ (integral of u_y , Eq.(25)) is available if

$$A = \frac{\alpha}{\delta}. \quad (26)$$

Since A is an arbitrary constant, we may choose A as in (26). With this choice, the general solution is

$$u(y) = -\delta e^{C_1} e^{-e^{y/\delta}} + C_2.$$

If $u(0) = 0$, and $u(\infty) = V_0$, then the constants C_1 and C_2 are

$$C_2 = V_0,$$

and

$$\delta e^{C_1} = V_0 e^1.$$

We get the solution for $u(y)$ that we call a turbulent solution U_T as:

$$U_T = V_0 \left(1 - e^{1 - e^{y/\delta}}\right),$$

that is limited, $u(0) = 0$, $u(L/2) \cong V_0$, and is acceptable.

4.4 Case of the Negative Sign in the Exponent

Again recall Eq.(19) and putting the solution for v there, we have:

$$\alpha u_{yy} + A(1 - e^{-\frac{y}{\delta}})u_y - p_x = 0, \text{ where } p_x = 0, \text{ as we seek a solution of a homogeneous equation.}$$

$$\frac{\alpha u_{yy}}{u_y} = A(1 - e^{-\frac{y}{\delta}}),$$

Solution for u_y :

$$\ln u_y = Ay + A\delta e^{-\frac{y}{\delta}} + C$$

or

$$\ln u_y = A\delta(\frac{y}{\delta} + e^{-\frac{y}{\delta}}) + C, \text{ and}$$

$$u_y = \exp(A\delta(\frac{y}{\delta} + e^{-\frac{y}{\delta}})) = D \exp(\frac{y}{\delta} - e^{\frac{y}{\delta}}).$$

$$u = \int \exp(A\delta(\frac{y}{\delta} + \exp(-\frac{y}{\delta})))dx = A_1 [\exp(\frac{y}{\delta} + \exp(\frac{y}{\delta})) - Ei(\exp(-\frac{y}{\delta}))] + A_2.$$

As $u(0) = 0$, then $A_2 = 0$ and solution u is the following:

$$u = A_1 \left[e^{\frac{y}{\delta} + e^{\frac{y}{\delta}}} - Ei(e^{-\frac{y}{\delta}}) \right], \quad (27)$$

where $Ei(x)$ is the integral exponential function. This solution for u grows indefinitely, so it is not physical, and will be disregarded.

5 General Solution for the Turbulent Flow

The general solution is proposed as a linear superposition of two solutions, laminar and turbulent:

$$U_{GHE} = \gamma U_T + (1 - \gamma)U_L, \quad (28)$$

where the coefficients γ and $(1 - \gamma)$ are introduced, to get V_0 at the center line. The first term containing U_T grows superexponentially in the boundary layer, while the second term containing U_L is nearly zero. Outside the boundary layer, the first term is constant, and the second term starts to grow (see Figure 7).

We get

$$U_{GHE} = V_0 \left[\gamma \left(1 - e^{1 - e^{y/\delta}} \right) + (1 - \gamma)4y(L - y)/L^2 \right]. \quad (29)$$

The value of γ can be calculated from the Eq.(19) at some point, better for small y , for example, $y = \delta$.

Substituting the solution U_{GHE} into Eq.(19) we get

$$\alpha U_{GHE,yy}(\delta) - v(\delta)U_{GHE,y}(\delta) = p_x \quad (30)$$

or, dropping the argument δ , and substituting the expression of U_{GHE1} from Eq.(28):

$$\alpha(\gamma U_{T,yy} + (1 - \gamma)U_{L,yy}) - v(\gamma U_{T,y} + (1 - \gamma)U_{L,y}) = p_x,$$

or

$$\gamma(\alpha(U_{T,yy} - U_{L,yy}) - v(U_{T,y} - U_{L,y})) + \alpha U_{L,yy} - v U_{L,y} = p_x,$$

and

$$\gamma = (p_x - \alpha U_{L,yy} + v U_{L,y}) / (\alpha (U_{T,yy} - U_{L,yy}) - v (U_{T,y} - U_{L,y})) \quad (31)$$

evaluated at $y = \delta$. Here $U_{T,yy}$ and $U_{L,yy}$ are the 2nd partial derivatives of U_T and U_L in y , $U_{T,y}$ and $U_{L,y}$ are the first partial derivatives of U_T and U_L in y , $v(y)$ is calculated using the Eq.(22) with A from Eq.(26), $p_x = -8V_0/(ReL^2)$.

The parameter δ and the value of γ in the comparisons with the experiments below will be chosen to fit the experimental data, as we do not have the material property τ^* for particular liquids used in the experiments, as $\delta = \sqrt{\tau^* \nu} / L$. The value of γ can be calculated from the parameters of experiments using Eq.(31) if the values of $V_0 = \frac{1}{2} Re p_x$ and L are known.

Each of the two solutions has different similarity parameters. The laminar parabolic solution depends on the Re number, while the turbulent solution depends on the parameter $\delta = \sqrt{\tau^* \nu} / L$.

The parameter τ^* (dimension of time) is a mean time between particle collisions. For gases this mean time between collisions can be calculated using hard-sphere model of particles at pressure p , and viscosity μ as $\tau^* = \Pi \mu / p$, where Π is a constant, $\Pi = 0.786$ [4]. For liquids this is more complicated (see [2], p.324 discussion about Frenkel work [16]), there is no explicit formula, and the experimental measurements are needed. It can be found by fitting the experimental velocity data (as will be shown in the next Sections) finding δ . Then τ^* can be found as $\tau^* = \delta^2 L^2 / \nu$.

6 Comparison of Analytical Solution with Experiments

6.1 Pipe Flow Experiment by Van Doorne at Re=720

Here a comparison will be provided for the approximate GHE and other analytical solutions with the pipe flow data Van Doorne 2004, 2007 [5, 6] (Prof. Bruno Eckhardt group). The analytical solution was obtained for 2D flow in Cartesian coordinates, but still we try it for pipes (cylindrical coordinates) assuming that in the vicinity of the wall it will work. Figure 3 shows the experimental data digitized from [5], and a number of different plots from (a) laminar (parabolic) flow profile (green line); (b) turbulent solution (blue line) and and (c) GHE solution. The figure demonstrates that neither the laminar nor turbulent solution fit the data, but the superposition U_{GHE} provides an excellent fit to the experimental mean velocity profile for $\gamma=0.66$ and $\delta=0.047$, and δ is assumed to be a Kolmogorov length scale. In [11] the GHE solution compared well with the experiment for the driven cavity flow [20], and the dimensional value of $\delta = 0.58mm$ was a good approximation to the experimentally observed "Kolmogorov microscale" $\delta_{exp} = 0.5mm$ ([20], p. 398).

The next Figure 4 is a comparison of the values of experimental turbulent intensity for horizontal velocity rms(u') with the corresponding analytical turbulent intensity. As the solution of the unsteady equations is not provided (not possible analytically), it is suggested that a turbulence is the oscillation between different stationary solutions, two solutions in our case, the laminar (parabolic) velocity profile U_L and the turbulent one given by U_T . Therefore, the rms(u') at every point is

$$rms(u') = \sqrt{\frac{\sum (U_m - u(t_n))^2}{N}}$$

where $U_m(y)$ is a mean velocity, $u(y, t_n)$ is a velocity at time t_n , and N is the number of measurements.

The analytical rms(u') was presented as a difference between two solutions U_T and U_L :

$$rms(u') = | \theta \cdot U_T - \beta \cdot U_L | \quad (32)$$

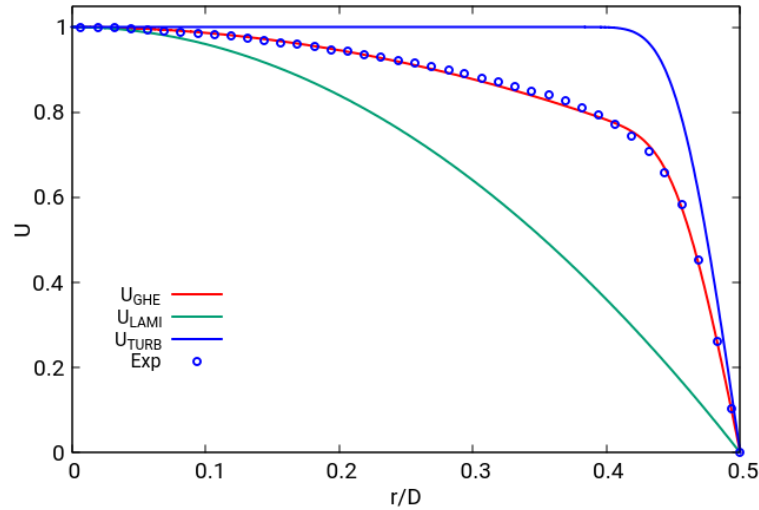


Figure 3: A comparison of experimental data for horizontal velocity by Van Doorne(2007) [5], water at $Re=720$, with the GHE model. The GHE solution which is the linear superposition of the turbulent and lamina profiles (U_{GHE} on the plot) fits the experimental velocity profile.

and shown in Figure 4. As one can see, the data and analytical curve are in concordance. The parameters of the analytical curve that define the difference of U_T and U_L are the following: $\theta = 3.552, \beta = 2.736, \delta = 0.047$.

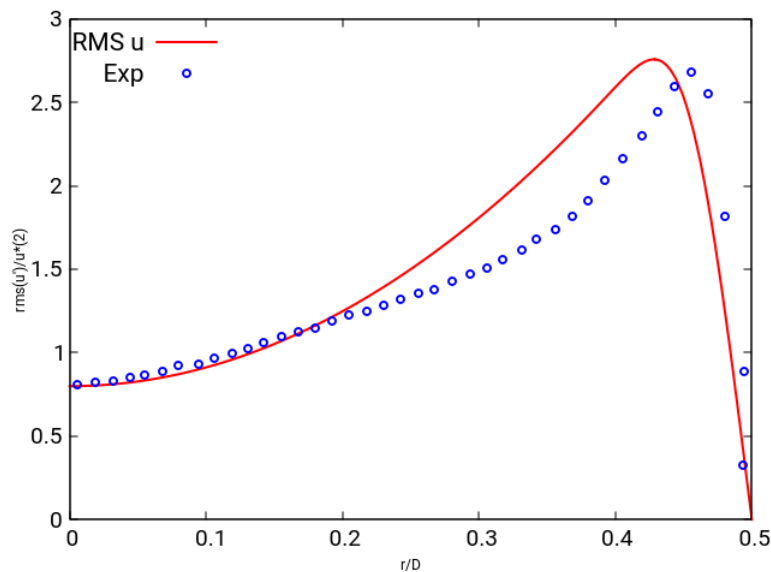


Figure 4: Comparison of experimental $rms(u')$ data [5] (blue circles) turbulent intensities and analytical solution from GHE (red curve). The comparison is quite satisfactory.

6.2 Experiments by Wei and Willmarth

For the experiments with a turbulent boundary layer, the velocity U^+ plots versus y^+ does not depend on Re number, see e.g. data from Wei and Willmarth (1989) [24], Figure 5. The parameter

$y^+ = \frac{yu_\tau}{\nu}$ where u_τ is so called friction velocity, y is the absolute distance from the wall, and ν is a kinematic viscosity. One can interpret y^+ as a local Reynolds number. The velocity scale u_τ is defined as $u_\tau = \sqrt{\frac{\tau_w}{\rho}}$, where wall shear stress τ_w , $\tau_w = \rho\nu \frac{dU}{dy}$ at $y=0$, and the dimensionless velocity is given by $u^+ = \frac{u}{u_\tau}$.

The analytical solution U_{GHE} is presented in Figure 5 as red line, and is in a good concordance with data (parameters are $\delta = 0.052$, $\gamma = 0.65$).

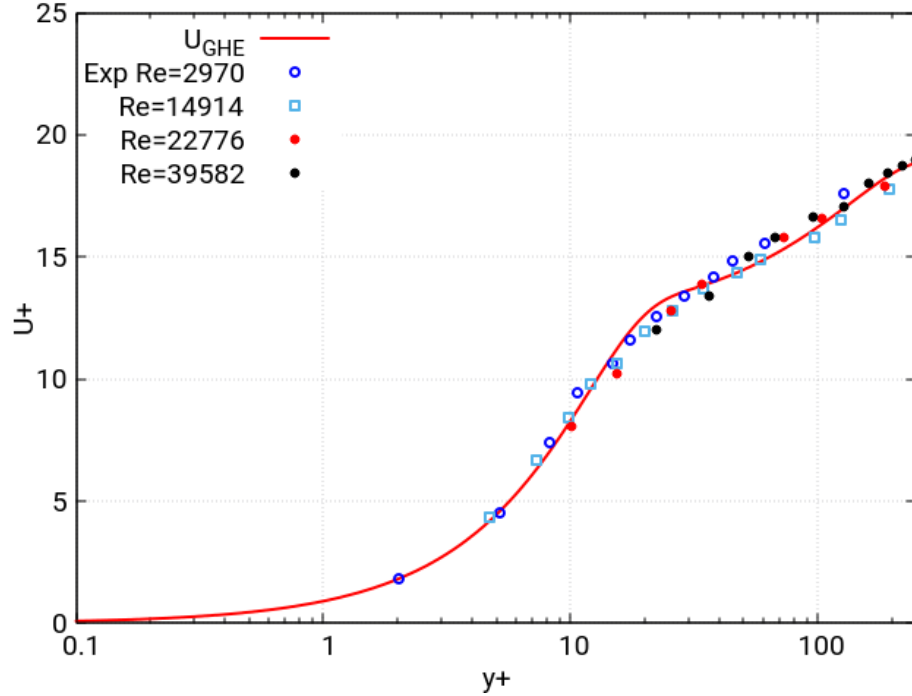


Figure 5: Mean velocity profiles in turbulent boundary layer from experiment [24] (distilled water), non-dimensionalized on inner variables, for the four Reynolds numbers examined. $Re = 2970$ (circles); $Re = 14914$ (squares); $Re = 22776$ (red dots); $Re = 39582$ (black dots), distilled water. The data for different Re numbers merge well in coordinates u^+, y^+ . The red line is an approximate GHE solution.

Typically, Figure 5 and Figure 7, the inner boundary layer (BL) region (viscous sublayer) is in the range $0 < y^+ < 5$, where $u^+ = y^+$ (blue line in Figure 7). The near-middle (buffer) BL region is in the range $5 < y^+ < 30$, a strictly nonlinear region. The far-middle (inner) BL region is in the range $30 < y^+ < 200$. Velocity profile in this region can be expressed as the logarithmic “law-of-the-wall” von Karman law

$$U^+ = 1/k \log y^+ + B, \quad (33)$$

$k = 0.41$, $B = 5.2$ (green line in Figure 7).

The outer (non-linear, essentially inviscid) region starts at $y^+ > 200$ and continues to the center line.

The analytical solution U_{GHE} fits well to the experimental data in all the regions (Figure 7, red line).

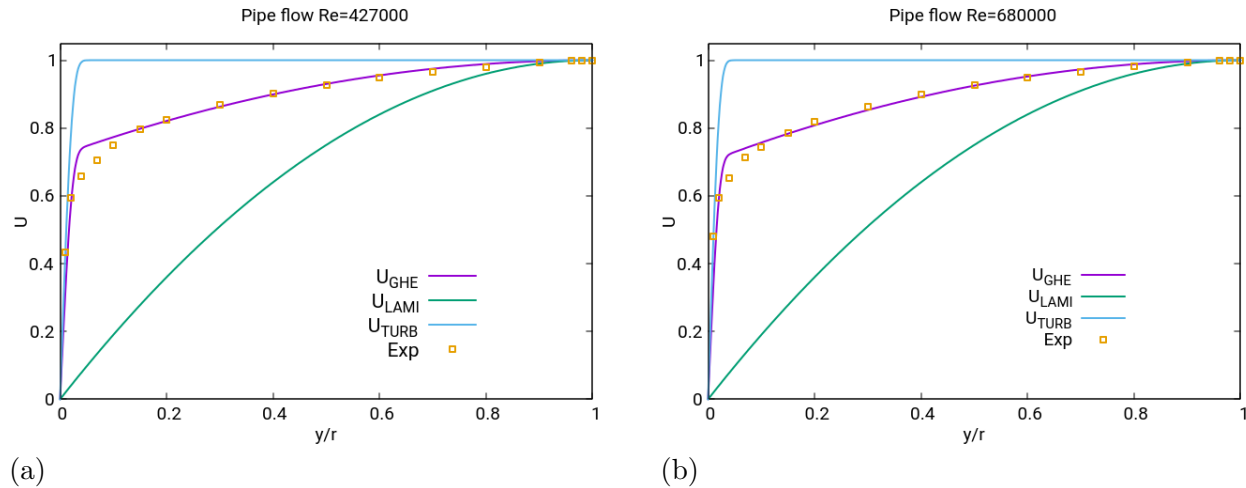


Figure 6: Experimental data for mean velocity profiles by horizontal velocity Nikuradse [21] for $Re=427,000$ (a) and $Re=970,000$ (b) compared to laminar flow profile (green), Turbulent flow profile (blue) and analytical solution GHE flow profile (purple). Approximate analytical solution U_{GHE} (purple curve) compares well with the experimental data (circles).

6.3 Experiments by Nikuradse for High Reynolds Numbers

The solution superposition principle works well for higher values of Reynolds number, up to nearly 10^6 , a range of nearly 3 orders of magnitude. Nikuradse (1932, 1933) (Prandtl group) experiments have been done for Re from 27,000 to $Re=970000$ [21, 22]. We present a comparison for $Re=427,000$ and $Re=970,000$ in Figure 6. The approximate analytical solution U_{GHE} (pink curve) compares well with the experimental data. The parameters for the analytical solution are the same for all the cases in [21], $\gamma = 0.71$, $\delta = 0.010$.

7 Discussion

Let us consider the turbulent boundary layer regions, the linear and the logarithmic “law-of-the-wall” von Karman law parts. Let us represent the turbulent boundary layer profile, Figure 7, where the components of GHE with the appropriate coefficients from Eq. (28) are plotted: the turbulent solution U_{1T} and the laminar solution U_{2L} , were added. The plot also has the log law by von Karman (the coefficients have been calculated by Nikuradse using his data [21]), linear law and empirical 1/7 power law, that was proposed first by Nikuradse [21].

The linear law is in the range $0 < y^+ < 5$, where the parabolic profile U_{2L} (laminar solution) is very small, and the turbulent solution for small y/δ becomes

$$U_T = V_0\gamma \left(1 - e^{-y/\delta}\right) = V_0\gamma \left(1 - e^{-1-(1+y/\delta)}\right) = V_0\gamma \left(1 - e^{-y/\delta}\right) = V_0\gamma (1 - (1 - y/\delta))$$

or

$$U_T = V_0\gamma y/\delta, \quad (34)$$

that is a linear law.

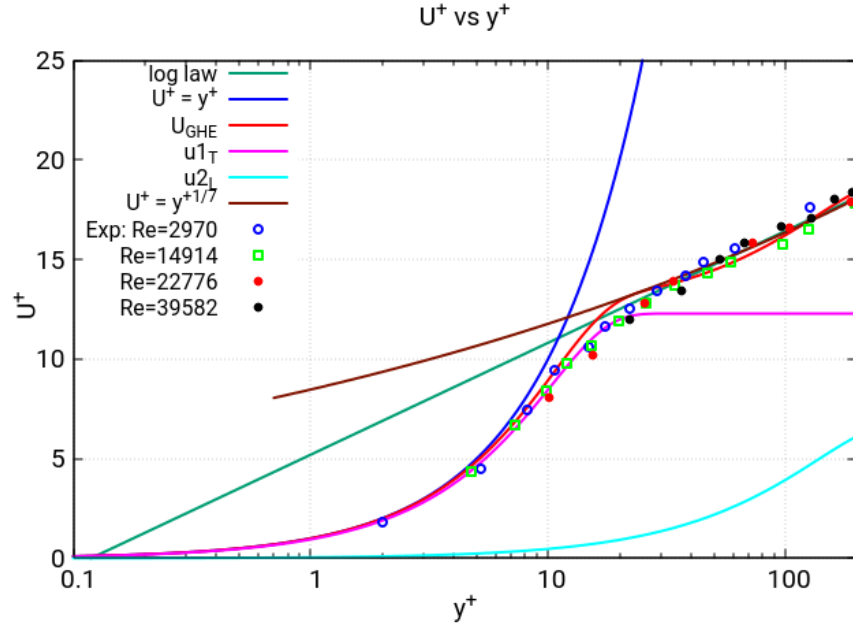


Figure 7: Velocity profiles in turbulent boundary layer: analytical solution U_{GHE} (red line) and its constituents, the turbulent solution U_{1T} and the laminar solution U_{2L} ; log law by von Karman $U^+ = 1/k \log y^+ + B$, $k = 0.41$, $B = 5.2$ (green line), linear law $U^+ = y^+$ (blue line) and empirical power law $U^+ = y^{+1/7}$ (brown), and experimental data (dots) by Wei and Willmarth (1989)[24].

In the range of $30 < y^+ < 200$, the solution U_{1T} becomes nearly constant ≈ 12.5 (pink line in Figure 7), and the GHE solution changes due to the growth of the laminar solution U_{2L} (cyan color line in Figure 7). That $u^+ = (12.5 + \log U_{1L})$, the parabolic solution would fit well into logarithmic “law-of-the-wall” (von Karman law). The empirical 1/7 power law, that was first proposed by Nikuradse, also fit well into the “law-of-the-wall”.

The parameter τ^* , a material property, if not known from the experiment for a given fluid, can be found by fitting the experimental velocity data (as we did in the previous Sections). In this case we will obtain the value of δ which will be used to calculate τ^* : $\tau^* = \delta^2 L^2 / \nu$.

Conclusions

The exact and approximate analytical solution of Generalized Hydrodynamic Equations (GHE) have been obtained for channel flow (that are valid for the pipe flow if $\delta \ll 1$), that constructed from two solutions for laminar and turbulent flows, presented as a linear superposition of these solutions.

The GHE solution for turbulent flows depends on two parameters: the Reynolds number Re , and $Al = \frac{\sqrt{\tau^* \nu}}{L} = \frac{\delta}{L}$, the Alexeev number (author of GHE and GBE). In Figure 7, the data for different Re numbers fall to a single law in (U^+, y^+) coordinates for the same kind of fluid. This data has the same Alexeev number Al if the same experimental dimensions hold. Changing the Al number (different fluid or dimensions) will produce different results.

The time parameter τ^* is a material property. For gases this is a mean time between collisions, and can be calculated for hard-sphere model of particles at pressure p , and viscosity μ as $\tau^* = \Pi \mu / p$, where Π is a constant, $\Pi = 0.786$. For liquids this is more complicated (see [2], p.324 discussion

about Frenkel work [16]), there is no explicit formula, and the experimental measurements are needed.

The approximate analytical solution for the GHE model has been compared with the experimental data for turbulent flows. The linear superposition of two solutions (turbulent and laminar) provides good agreement with the experimental axial mean velocity data in a wide range of Reynolds number from $Re=720$ to $Re = 960,000$.

The experimental data for turbulent intensities for axial velocity are in concordance with the analytical equation (weighted difference of the turbulent and laminar solutions). Apparently the turbulent oscillations are the oscillations between two solutions (two in considered case): the turbulent solution U_T and the laminar solution U_L . GHE intrinsically include a turbulence model.

Moreover, the obtained analytical solution was able to capture correct velocity behavior across the whole turbulent boundary layer (BL) and into the external flow: from the inner viscous sublayer to the outer layer of the turbulent BL. It also compares well with the experiments by Wei and Willmarth (1989).

The analytical solution presents the explicit verifiable proof that the Alexeev generalized hydrodynamic theory (GHE and GBE) is in good agreement with experiments for turbulent flows.

Availability of data

The data that support the findings of this study are available from the corresponding author upon reasonable request.

Acknowledgments

Author would like to extend the sincere thanks to Dr. Yuri Bozhkov for discussions of the text during manuscript preparation.

References

- [1] B. V. Alexeev, The generalized Boltzmann equation, generalized hydrodynamic equations and their applications. *Phil. Trans. Roy. Soc. London, A.* 349 (1994), 417-443.
- [2] Alexeev, B.V., *Generalized Boltzmann Physical Kinetics*, Elsevier, 2004.
- [3] J. Allegre, D. Bisch, J.C. Lengrand, *J. of Spacecraft and Rockets*, 34 (6), 724-728 (1997)
- [4] Cercignani C. *Theory and Application of the Boltzmann Equation*, Scottish Academic Press, Edinburgh and London, 1975.
- [5] C.W.H. Van Doorne, Jerry Westerweel, 2007, Measurement of laminar, transitional and turbulent pipe flow using Stereoscopic-PIV, February 2007, *Experiments in Fluids* 42(2), DOI: 10.1007/s00348-006-0235-5.
- [6] Casimir Willem Hendrik Van Doorne, *Stereoscopic PIV on transition in pipe flow*, Ph.D. Thesis, TU Delft, Netherlands, 2004.
- [7] Fedoseyev A.I., Alexeev, B.V. Mathematical model for viscous incompressible fluid flow using Alexeev equations and comparison with experimental data. In: Dey, S.K., Ziebarth, G., Ferrandiz (Eds.), *Proceedings of Advances in Scientific Computing Modelling (Special Proceedings of IMACS'98)*. Alicante, Spain, 1998, 158-163.

- [8] A. I. Fedoseyev, E. J. Kansa, C. Marin, M. Volz, and A. G. Ostrogorsky, AIAA Paper 2000-0698.
- [9] Fedoseyev A., A regularization approach to solving the Navier-Stokes Equations for Problems with Boundary Layer, *Comput. Fluid Dynamics J.*, 9, (2001) 317-324.
- [10] A. I. Fedoseyev, E. J. Kansa, C. Marin, and A.G. Ostrogorsky (2001) *Japanese Computational Fluid Dynamics Journal* 10(3), 325-333.
- [11] Fedoseyev A.I., Alexeev, B.V., Simulation of viscous flows with boundary layers within multiscale model using generalized hydrodynamics equations, *Procedia Computer Science*, 1 (2010)665-672.
- [12] Fedoseyev A., Alexeev B.V., Generalized hydrodynamic equations for viscous flows-simulation versus experimental data, in AMiTaNS-12, American Institute of Physics AIP CP1487, pp.241-247.
- [13] Fedoseyev A., Finite element method stabilization for supersonic flows with flux correction transport method, *AIP Conference Proceedings* 2302, 120003 (2020); <https://doi.org/10.1063/5.003351>
- [14] Fedoseyev A., Griaznov V., Simulation of Rarefied Hypersonic Gas Flow and Comparison with Experimental Data, in AMiTaNS-2021, Conf. Proc., AIP CP 2522, 100003, 2021, Ed. M.Todorov.
- [15] Fedoseyev A., Griaznov V., Ouazzani J., Simulation of rarefied hypersonic gas flow and comparison with experimental data II, *Proc. AMITANS-2022 Conf.*, AIP CP 2953, 2023, Ed. M.Todorov.
- [16] Frenkel', Ya.I. . *Kineticheskaya Teoriya Zhidkosti*, (Kinetic Theory of Liquids).1945 Izd. AN SSSR, Moscow-Leningrad.
- [17] Harvey J.K., Holden M. S., and Wadhams, T. P., Code Validation Study of Laminar Shock/Boundary Layer and Shock/Shock Interactions in Hypersonic Flow, Part B: Experimental Measurements," AIAA Paper 2001-1031, January 2001.
- [18] Holden, M. S., Wadhams, T. P., Candler, G. V., Harvey J. K., Measurements in Regions of Low Density Laminar Shock Wave/Boundary Layer Interaction in Hypervelocity Flows and Comparison with Navier-Stokes Predictions," AIAA Paper 2003-1131, January 2003.
- [19] J. Kim, S.J. Kline, and J. P. Johnston (1980) *ASME J. Fluids Engng.* 102, 302-308.
- [20] R. Koseff, R. L. Street, *Trans. ASME/Journal of Fluids Engineering* 106 (1984) 390-398.
- [21] J. Nikuradse, *Laws of Flow In Rough Pipes*, NASA Technical Memorandum 1292, 1950. Translation of *Stromungsgesetze in rauhen Rohren.*, VDI-Forschungsheft 361. Beilage zu *Forschung auf dem Gebiete des Ingenieurwesens* Ausgabe B Band 4, July/August 1933.
- [22] J. Nikuradse, *Laws of turbulent flow in smooth pipes* (English translation), NASA (1932) TT F-10: p. 359 (1966). Available from [https://www.Princeton.edu/mae/people/faculty/smits/homepage/data-1/nikuradse data/Nikuradse German_1932.pdf](https://www.Princeton.edu/mae/people/faculty/smits/homepage/data-1/nikuradse%20data/Nikuradse%20German_1932.pdf)

- [23] Polyanin A.D., Zaitsev V.F., Handbook of Exact Solutions for Ordinary Differential Equations, 2002, Chapman Hall, CRC Press Company, Boca Raton, London.
- [24] T. Wei ,W. W. Willmarth, Reynolds-number effects on the structure of a turbulent channel flow, J. Fluid Mech. (1989), vol 204, pp. 57-95.